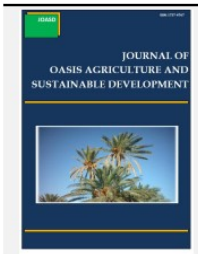

JOURNAL OF OASIS AGRICULTURE AND SUSTAINABLE DEVELOPMENT

www.joasdjournal.org

JOASD

p-ISSN: 2724 – 699X
e-ISSN: 2724-7007

Modeling the natural vegetation dynamic under climate change scenarios in coastal protected dryland of southeastern Tunisia

Abdelkader Idi [1,2+], Jamila Msadek [2+], Abderrazak Tlili[2] & Mohamed Tarhouni[2*]

[1] *Faculty of Sciences of Gabes. University of Gabes, Tunisia.*
[2] *Laboratory of Pastoral Ecosystems, Spontaneous Plants and Associated Microorganisms. Arid Regions Institute - University of Gabes – 4100 Medenine - Tunisia.*

Article info

Article history:
Received: 16 January 2024
Accepted: 21 February 2024

Keywords: Bioclimatic variables, Soil, Occurrence, Modeling, Radiometric index, Climate change

***Corresponding author**
medhtarhouni@yahoo.fr
[+]Equal Contribution

Conflict of Interest: The authors declare no conflict of interest.

Abstract

According to the Intergovernmental Panel on Climate Change (IPCC), climate change is mainly manifested by severe droughts and rainfall decrease. These effects are multiple and vary from one region to another around the world including rising temperatures, altered precipitation patterns and degradation of the natural flora. The Zarat region (Gulf of Gabes) is notable for its climate variation, shallow waters, high levels of temperature and salinity. Understanding the vegetation dynamics in this coastal protected region under climate change scenarios is important for projection to the whole ecosystems. The Maxent model is used to predict the potential distribution of plant groups and Soil Adjusted Vegetation Index (SAVI) classes for many future time-periods (2021-2040, 2041-2060, 2061-2080 and 2081-2100) under different climate change scenarios in the Zarat region. Main results indicate that variables related to precipitation and temperature are more significant for predicting plants and SAVI classes distributions. Our findings can provide scientific basis for the dryland sustainable management and for plant community's behavior under climate change.

1. INTRODUCTION

Vegetation is a vital component playing a crucial role in regulating the global carbon balance (Erb et al., 2018; Ge et al., 2021; Gao et al., 2022). Vegetation provides many of the essential ecosystem services. These last included soil stabilization, water regulation, carbon sequestration and grain production (Lü et al., 2012). Climate change can be considered as the primary force driving the dynamics of vegetation worldwide especially in the semiarid and arid regions (Zhang et al., 2018; Gao et al., 2022). This could lead to significant ecological and economic losses (Chen et al., 2020; Ge et al., 2021). Therefore, understanding the impacts of climate change on vegetation dynamics is crucial for developing effective strategies to mitigate these effects and ensure the long-term sustainability of our ecosystems. In addition to climate change, human activities, increasing the greenhouse gases emission into the atmosphere, such as deforestation and industry, are strongly affecting the structure and function of ecosystems (Ouled Belgacem & Louhaichi, 2013; Zhang et al., 2018; Tong et al., 2019). So, it is very interesting to protect the natural floristic resources for maintaining the ecological equilibrium/biodiversity and minimizing the impacts of climate change on wild ecosystems (Ding et al., 2016).

The monitoring of vegetation dynamics becomes easier thanks to the availability of remotely sensed imagery (Jewitt et al., 2015). Remote sensing is a powerful tool that allow researcher to analyse changes in less time, with lower cost, and more precision (Maina et al., 2020). The remote sensed data provide useful information for monitoring degraded lands and environmental changes (Kumar, 2022). These later result in radiance values, which can be detected through radiometric vegetation indices (Kumar, 2022). According to Lemenkova &

Debeir (2023), the vegetation index (VI) is a metric used to measure and monitor the health, density, and growth of plant cover. It can be calculated using various spectral bands of the electromagnetic spectrum, which are sensitive to the presence and the amount of chlorophyll pigments in leaves (Zeng et al., 2022). The Soil Adjusted Vegetation Index (SAVI) is recommended for dryland studies since it reduces the impact of soil brightness on spectral vegetation indices and helps to indicate the areas where vegetation is decreasing (Almutairi et al., 2013; Lemenkova & Debeir, 2023).

In these contexts, the present study aims to monitor the future evolution of natural vegetation cover under two climatic change scenarios through radiometric and remotely sensed indices as well as some plant groups characteristics in the Zarat region. The main occupations are about how does the climate change influenced the vegetation cover in coastal area of North Africa? How can the Shared Socioeconomic Pathways (SSP) scenarios be used to predict the effects of climate change on radiometric vegetation indices?

2. MATERIAL AND METHODS

2.1. Study area

The study was conducted in the coastal and protected area of Zarat region (33°40'N, 10°23'E, Gulf of Gabes, Tunisia) (Fig.1).

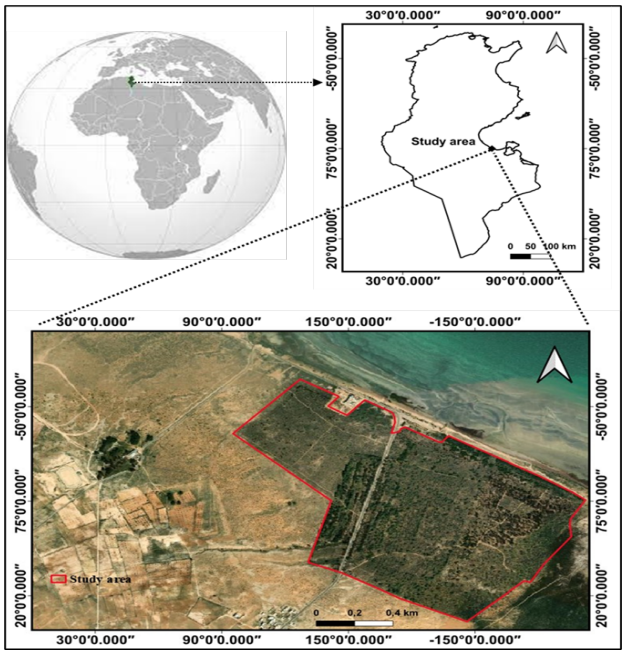

Fig. 1. Geographical location of the study region.

The climate is arid with mild winters (Medini-Bouaziz et *al*., 2017). Rainfall is irregular and varied between 100 and 200 mm per year (Genin et *al*., 2006). According to these authors, the mean annual temperatures are usually high and varied between 15°C and 20°C. Three plant groups, called G1–G3, are founded in the study area: G1: *Rhanterium suaveolens* (Desf.) and *Lygeum spartum* (L.); G2: *Lycium shawii* (Roem. & Schult) and *Nitraria retusa* (Forssk.); G3: *Imperata cylindrica* (L.).

2.2. SAVI index

The Soil Adjusted Vegetation Index (SAVI) is introduced by Huete (1988) as:

$$SAVI=(NIR-Red)/(NIR+Red+L) \times (1+L)$$

where L is a correction factor which ranges from 0 (very high vegetation cover) to 1 (very low vegetation cover). The most typically used value is 0.5 which is for intermediate vegetation cover (Xue & Su, 2017). NIR (near-infrared) and Red are the spectral band values. These last are downloaded from Climate Engine platform (www.climateengine.org) accessed on March 2018 which represents the vegetation growing season during very rainy year in the retained study area. The downloaded satellite image comes from the Sentinel-2 dataset accessible from the European Space Agency. After calculation, the obtained map is categorized into three classes depending on the SAVI values: 'high' (0.3-1), 'medium' (0.2–0.3) and 'low' (<0.2) using QGIS 3.30.3 software..

2.3. Data modeling approach

The 19 basic climatic data of the time-periods 2021-2040, 2041-2060, 2061-2080 and 2081-2100 are obtained from the "WordClim" database (www.worldclim.org) at a ground resolution of 30 arc-seconds (≈1 km²/pixel). Three topographical variables (elevation, exposure, slope) are also taken from this same database. In addition to these data, 12 soil variables are downloaded from the soil-grids database (www.soilgrids.org, 250 m resolution). Indeed, a total of 34 variables is used to model the current and the future situations of the three above-mentioned plant groups and SAVI classes (Table 1). All these variables are re-sampled to 30 m resolution using QGIS. The occurrences points of each plant group and each SAVI class are obtained using regular points tool in QGIS with 50m space. These points are randomly subdivided into two major subsets. The first one, containing 75% of the records, is used as training data to build the distribution model. The second one, containing 25% of points, is used to test and validate the model. The maximum entropy algorithm "MaxEnt", open-source

computer program that runs under JAVA, is used for modeling. This model represents an important prediction tool in conservation ecology (Phillips et al., 2004).

Two greenhouse gases emission scenarios (Shared Socioeconomic Pathways, SSP) are considered from the General Circulation Model (GCM) of the Canadian Earth System Model version 5 (CanESM5): the lowest (SSP245) and the most extreme emission scenario (SSP585). These SSPs are adopted by the Fifth Assessment Report (IPCC, 2014).

2.4. Model performance

The Receiver Operating Characteristic (ROC), showed by the Area Under Curve (AUC), is used to validate the predictive capacity of the model. AUC is a measure of model performance, and its higher value is close to one (1), the greater it deviates from a random pattern (Phillips et al., 2004). According to the proposal of Elith (2006), the AUC values are interpreted as follows: the model is "excellent" if AUC > 0.90; "good" if 0.80 < AUC ⩽ 0.90; "acceptable" if 0.70 < AUC ⩽ 0.80; "bad" if 0.60 < AUC ⩽ 0.70; and "invalid" if AUC ⩽ 0.60. The Jackknife procedure (regularized training gain) and percent variable contributions are used to determinate the predictive power of each variable and to identify those that contribute most in the distribution model produced by MaxEnt (Yost et al., 2008).

Table 1. General description of the studied bioclimatic, soil and topographic variables.

Data sources	Variables	Description	Unit
Worldclim (Bioclimatic data)	bio1	Mean annual temperature	°C
	bio2	Mean diurnal range	°C
	bio3	Isothermality	-
	bio4	Temperature seasonality	°C
	bio5	Max temperature of the warmest month	°C
	bio6	Minimum temperature of the coldest month	°C
	bio7	Temperature annual range	°C
	bio8	Mean temperature of the wettest quarter	°C
	bio9	Mean temperature of the driest quarter	°C
	bio10	Mean temperature of the warmest quarter	°C
	bio11	Mean temperature of the coldest quarter	°C
	bio12	Annual precipitation	mm
	bio13	Precipitation of the wettest month	mm
	bio14	Precipitation of the driest month	mm
	bio15	Precipitation seasonality	mm
	bio16	Precipitation of the wettest quarter	mm
	bio17	Precipitation of the driest quarter	mm
	bio18	Precipitation of the warmest quarter	mm
	bio19	Precipitation of the coldest quarter	mm
Soilgrids (Soil data)	Bulk dens	Bulk density	
	Cation	Depth: 0-5	
	Clay content	Depth: 0-5	
	Coarse	Depth: 0-5	
	Nitrogen	Depth: 0-5	
	Organic carbon dens	Organic carbon density	
	pH water	Depth: 0-5	
	Sand	Depth: 0-5	
	Silt	Depth: 0-5	
	Soil organic carbon	Depth: 0-5	
	Soil organic carbon stock	Depth: 0-3	
Worldclim (Topographic data)	Elevation	Elevation	m
	Slope	Slope	degree
	Aspect	Aspect	degree

To carry out the necessary maps, the ASCII files generated by MaxEnt are analyzed by QGIS to show the evolution of the SAVI classes and plant groups distribution under the tested scenarios. Each of the above-mentioned SAVI classes is categorized into 4 sub-classes as follow: area with low value (0–0.25), moderate value (0.25–0.50), high value (0.50–0.75), and very high value (0.75-1). Of course, the most important sub-classes for the analysis are the very high ones for each SAVI class.

3. RESULTS & DISCUSSION

3.1. Model validation, variables' contribution, and SAVI evolution

It is clear from Table 2 that the AUC, which measure the prediction accuracy of the model, is ranging from 0.839 to 0.857 and confirms the good performance and robustness of the model for the high class of SAVI in Zarat. The degree to which a model can successfully discriminate occurrence from background locations has been suggested to be associated with high AUC values (Lobo et *al*., 2008). It is important to mention that AUC indicates significantly higher accuracy of the model when compared to random prediction. The 0.5 value represents the completely random prediction (Massada et *al*., 2012).

Table 2. Area Under Curve (AUC) of the very high value sub-class (0.75-1) for different SAVI classes (High, Medium, Low) under current (2018) and future climate scenarios (SSP245, SSP585) from 2021 to 2100 in Zarat protected area.

		High	Medium	Low
2018		0.847	0.630	0.522
SSP245	2021-2040	0.841	0.629	0.529
	2041-2060	0.857	0.626	0.523
	2061-2080	0.853	0.629	0.523
	2081-2100	0.839	0.625	0.527
SSP585	2021-2040	0.857	0.632	0.527
	2041-2060	0.849	0.628	0.526
	2061-2080	0.844	0.623	0.526
	2081-2100	0.851	0.637	0.530

Under both scenarios (SSP245 and SSP585) from the CanESM5 model, the contribution percent of variables (Fig.2) shows that data related to topography (Aspect, Elevation and Slope), mean temperature of the coldest quarter (bio11), carbon stock, pH water and coarse were the strongest predictor of high SAVI (4.9%, 11.57%, 7.15%, 16.57%, 30.2%, 6.97% and 5.3% respectively for SSP245 and 4%, 12.42%, 6.05%, 13.35%, 27.00%, 5.3% and 4.52% for SSP585). Concerning medium SAVI, precipitation of the driest month (bio14; 7.97% and 6.62% respectively for SSP245 and SSP585), precipitation of the warmest quarter (bio18; 11.42% and 14.65%), elevation (36.50% for both SSP245 and SSP585) and some soil related variables (carbon stock (9.05% and 5.42%) and Coarse (11.92% and 10.95%)) are the best predictors. It seems that carbon stock (72.92% and 77.30% respectively for SSP245 and SSP585) is the main factor influencing the low SAVI class. Some studies showed that distribution of plant species is influenced by elevation (Dülgeroğlu & Aksoy, 2019). There are some species that migrate toward elevated habitats to reach more suitable conditions for their development (Parmesan & Yohe, 2003). Moreover, variables related to soil characteristics are highlighted by many researchers for their importance in plant species distribution (Piri Sahragard & Ajorlo, 2018). The MaxEnt model predicts the distribution of SAVI and shows differences from the present occurrences. Mainly the environmental conditions are involved in such dynamic.

The results of the current and projected areas of SAVI classes are showed in Tables 3 and 4. When looking at current climatic, edaphic, and topographic variables, we found that model produced 98.23ha (56.76%), 117.87ha (68.11%) and 0ha respectively for the (0.75-1) sub-class of high, medium, and low SAVI (Table 3). Under SSP245 and SSP585 climate scenarios, edaphic and topographic variables increased the sub-class (0.75-1) of high SAVI with a percentage about 30% (Table 4). This indicates positive growth and potential for the conservation of plant species inside the protected area in the future. Fencing is a primary management practice for the conservation of rangeland plant communities since it promotes flora regeneration (Tarhouni et *al*. 2017). Such changes are followed by higher vegetation cover as indicated by SAVI in some new habitats in the protected area. However, the medium SAVI class showed a decline under SSP585 during 2041-2060 (-7.03%) and 2061-2080 (-12.61%) (Table 4). The unfavorable environmental conditions associated with the SSP585 scenario are likely to have adverse impacts on vegetation vigor and potential loss of vegetation cover. These effects could lead to a decline of SAVI.

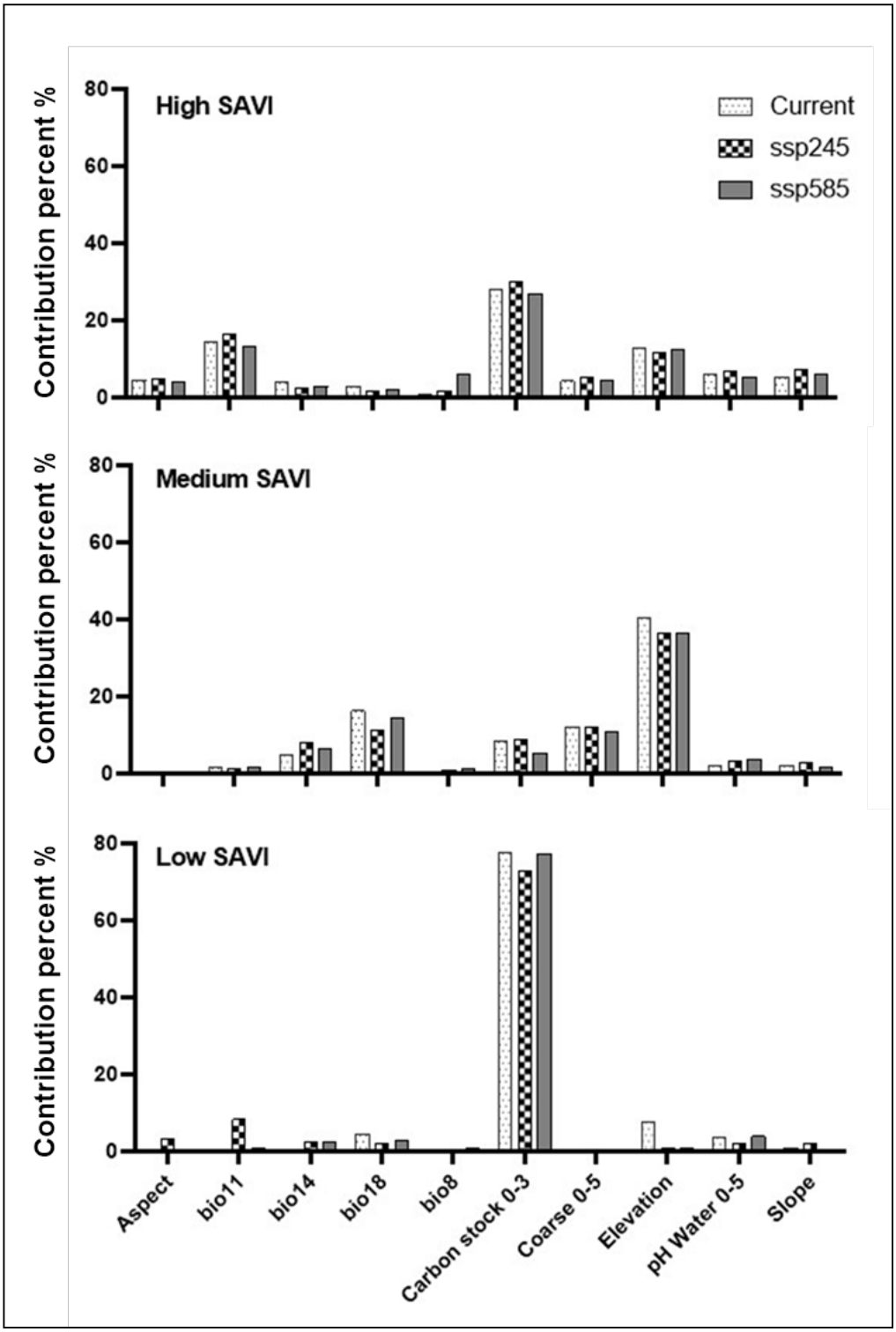

Fig. 2. Contribution percent (%) of climatic, edaphic, and topographic variables to Maxent model for SAVI classes (Low, Medium, High).

Table 3. SAVI area (ha, %) during the different time-periods and according to the SSP245 and SSP585 scenarios from the CanESM5 model. The most important sub-classes for the analysis (for each SAVI class) are indicated **in Bold**.

		Sub-classes	High	Medium	Low
2018		**0 - 0.25**	9.27 (5.35%)	0 (0%)	0
		0.25 - 0.50	22.63 (13.08%)	0 (0%)	68.05 (39.32%)
		0.50 – 0.75	42.95 (24.82%)	55.20 (31.89%)	105.02 (60.68%)
		0.75 - 1	**98.23 (56.76%)**	**117.87 (68.11%)**	**0**
SSP245	**2021-2040**	**0 - 0.25**	15.69 (9.06%)	0 (0%)	7.77 (4.49%)
		0.25 - 0.50	11.20 (6.47%)	0 (0%)	165.30 (95.51%)
		0.50 – 0.75	18.30 (10.57%)	43.17 (24.95%)	0 (0%)
		0.75 - 1	**127.88 (73.89%)**	**129.90 (75.05%)**	**0 (0%)**
	2041-2060	**0 - 0.25**	16.96 (9.80%)	0 (0%)	80.23 (46.35%)
		0.25 - 0.50	13.15 (7.59%)	0 (0%)	92.84 (53.65%)
		0.50 – 0.75	18.75 (10.83%)	53.41 (30.86%)	0 (0%)
		0.75 - 1	**124.22 (71.78%)**	**119.66 (69.14%)**	**0 (0%)**
	2061-2080	**0 - 0.25**	18.08 (10.44%)	0 (0%)	10.53 (6.09%)
		0.25 - 0.50	9.11 (5.27%)	0 (0%)	162.54 (93.91%)
		0.50 – 0.75	13.37 (7.73%)	54.60 (31.55%)	0 (0%)
		0.75 - 1	**132.51 (76.57%)**	**118.47 (68.45%)**	**0 (0%)**
	2081-2100	**0 - 0.25**	12.47 (7.21%)	0 (0%)	26.52 (15.32%)
		0.25 - 0.50	15.09 (8.72%)	173.07 (100%)	146.55 (84.68%)
		0.50 – 0.75	15.54 (8.98%)	0 (0%)	0 (0%)
		0.75 - 1	**129.97 (75.10%)**	0 (0%)	0 (0%)
SSP585	**2021-2040**	**0 - 0.25**	21.51 (12.43%)	0 (0%)	28.61 (16.53%)
		0.25 - 0.50	8.29 (4.73%)	0 (0%)	144.46 (83.47%)
		0.50 – 0.75	10.68 (6.17%)	34.06 (19.68%)	0 (0%)
		0.75 - 1	**132.59 (76.61%)**	**139.01 (80.32%)**	**0 (0%)**
	2041-2060	**0 - 0.25**	13.22 (7.64%)	0 (0%)	12.10 (6.99%)
		0.25 - 0.50	13.89 (8.03%)	0 (0%)	160.97 (93.01%)
		0.50 – 0.75	17.63 (10.19%)	63.49 (36.68%)	0 (0%)
		0.75 - 1	**128.33 (74.15%)**	**109.58 (63.32%)**	**0 (0%)**
	2061-2080	**0 - 0.25**	14.12 (8.16%)	0 (0%)	24.80 (14.33%)
		0.25 - 0.50	16.36 (9.45%)	0 (0%)	148.27 (85.67%)
		0.50 – 0.75	23.01 (13.29%)	70.06 (40.48%)	0 (0%)
		0.75 - 1	**119.59 (69.10%)**	**103.01 (59.52%)**	**0 (0%)**
	2081-2100	**0 - 0.25**	10.53 (6.09%)	0 (0%)	22.19 (12.82%)
		0.25 - 0.50	13.82 (7.98%)	0 (0%)	150.88 (87.18%)
		0.50 – 0.75	15.98 (9.24%)	44.22 (25.55%)	0 (0%)
		0.75 - 1	**132.74 (76.69%)**	**128.85 (74.45%)**	**0 (0%)**

Table 4. Change in area (ha, %) of the most important sub-classes (0.75-1) of SAVI values (high, medium, low) from the currently to future time-periods under the SSP245 and SSP585 climate change scenarios.

		Area (ha)			Percent change (%)		
		High	Medium	Low	High	Medium	Low
2018	**Current**	98.23	117.87	0	0	0	0
2021-2040	**SSP245**	127.88	129.90	0	30.18	10.21	0
	SSP585	132.59	139.01	0	34.98	17.94	0
2041-2060	**SSP245**	124.22	119.66	0	26.46	1.52	0
	SSP585	128.33	109.58	0	30.64	-7.03	0
2061-2080	**SSP245**	132.51	118.47	0	34.90	0.51	0
	SSP585	119.59	103.01	0	21.74	-12.61	0
2081-2100	**SSP245**	129.97	107.43	0	32.31	-8.86	0
	SSP585	132.74	128.85	0	35.13	9.32	0

3.2. Model validation, variables contribution, and plant groups dynamic

The AUC of the three plant groups (G1, G2 and G3) indicates excellent accuracy of prediction (AUC ranges from 0.98 to 1) (Table 5). Hence, the model is classified as satisfactory with the given set of training and test data.

The contribution of climatic, edaphic, and topographic variables in Maxent of G1 (Fig.3) showed that bio1 (6.3 and 6.8% respectively for SSP245 and SSP585), bio3 (30.8 and 26.87%), bio8 (12 and 5.17%), bio14(12.1 and 8.32%) and bio18 (17.1 and 19.97%) are the highest followed by carbon stock (7.07 and 4.25%) and aspect (3.24 and 4.3%). Regarding G2, the percentage of variables contribution reveals that bio 18 is the highest (28.07 and 29.27% respectively for SSP245 and SSP585) followed by carbon stock (26.97 and 26%) and bio3 (21.27 and 22.35%). For G3, the carbon stock shows the highest percentage of contribution (47.45 and 54.3% respectively for SSP245 and SSP585). Since the distribution pattern of plants is closely linked to precipitation and temperature (Zhong et *al*., 2010), it seems that the soil carbon stock can be useful to predict future vegetation dynamic under climate change scenario.

Table 5. Area Under Curve (AUC) of the most important sub-class (0.75-1) for different plant groups; G1: *Rhanterium suaveolens* and *Lygeum spartum*; G2: *Lycium shawii* and *Nitraria retusa*; G3: *Imperata cylindrica* under current (2018) and future climate scenarios (SSP245, SSP585) from 2021 to 2100 in Zarat protected area.

		G1	G2	G3
2018		0.981	0.994	0.999
SSP245	**2021-2040**	0.982	0.993	1
	2041-2060	0.981	0.992	0.998
	2061-2080	0.982	0.993	0.999
	2081-2100	0.982	0.993	0.999
SSP585	**2021-2040**	0.983	0.993	0.999
	2041-2060	0.982	0.993	0.999
	2061-2080	0.981	0.994	0.998
	2081-2100	0.980	0.994	0.998

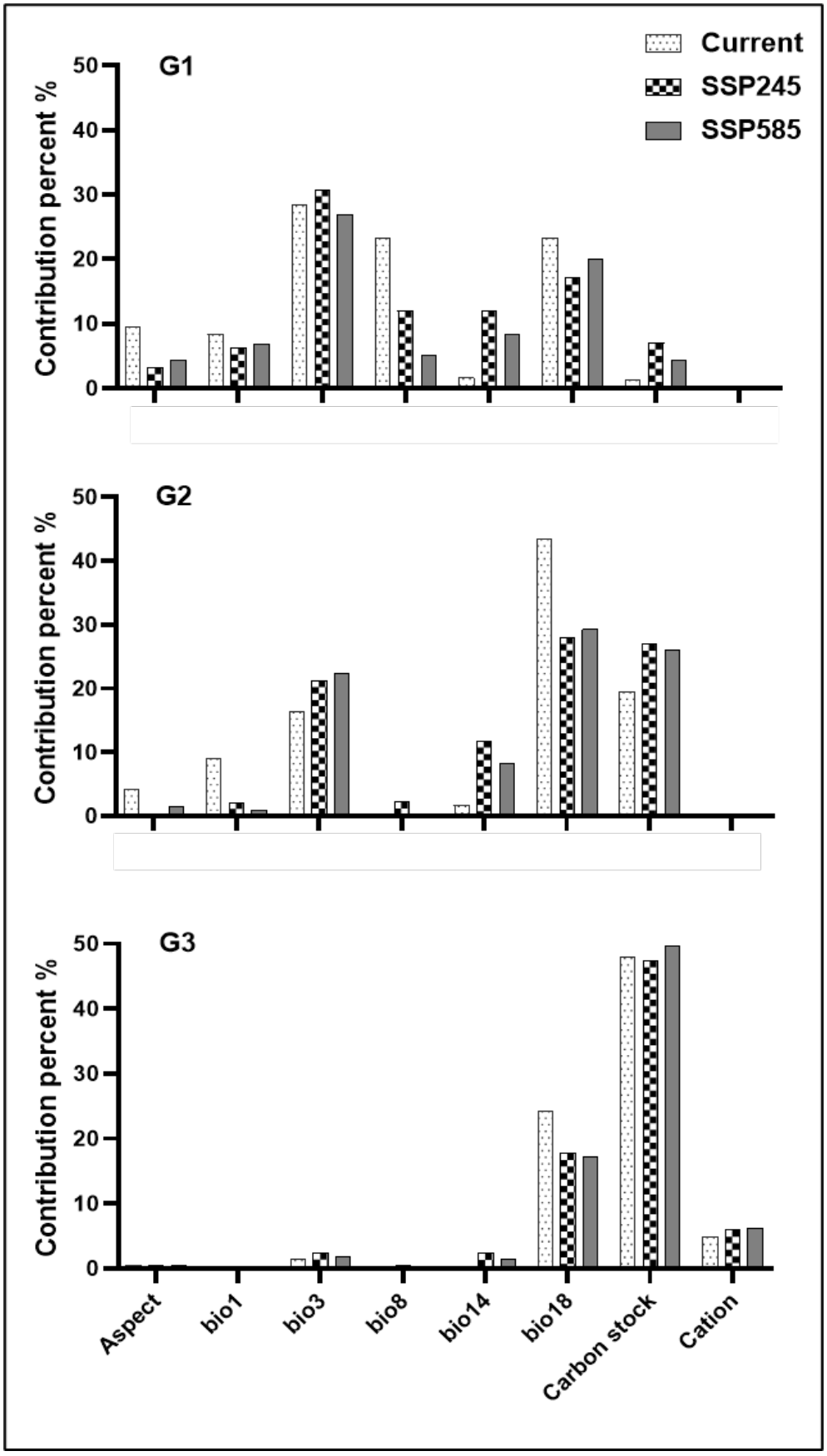

Fig. 3. Contribution percent (%) of climatic, edaphic and topographic variables to Maxent model for plant groups. G1: *Rhanterium suaveolens* and *Lygeum spartum*; G2: *Lycium shawii* and *Nitraria retusa*; G3: *Imperata cylindrica*.

Currently, the group 1 (*Rhanterium suaveolens* and *Lygeum spartum*) occupies a large area of 147ha (60.2%). The predicted areas of G1 in future time-periods according to the SSP245 and SSP585 scenarios does not differ significantly from the current one (changes ranging from -2.54 to 1.68% (Table 6)). It seems that plant group with a wide range of distribution are not heavily influenced by the variables of the prediction scenarios. It could also indicate that this group reached an equilibrium state. The model application shows a moderate distribution of G2 (*Lycium shawii* and *Nitraria retusa*) (77.46ha, 31.7%) in current situation (Table 6). In the future projections, percent of changes range from -16.98 to 6.75%. The oscillation in this plant group could be driven by the floristic composition which can be more adapted and tolerant to the environmental variability of the studied scenarios. Factors such as annual temperature and mean annual precipitation may influence the plant distribution. Temperature and precipitation are considered as the major determinants of plant distribution in a global scale (Zhao et *al*., 2018). At a local scale, the distribution of plants is consistently influenced by precipitation and temperature, with precipitation being the primary factor that controls plant productivity and composition (Ben Mariem & Chaieb, 2017). This finding would suggest that the G2 plant group is adapted to the variation of environmental conditions of the protected area. Indeed, plant groups are undergoing natural change as the ecosystem progress towards a more stable state especially in the context of climate change (Gann et *al*., 2019). The actual area of G3 (*Imperata cylindrica*) is 19.5ha (8%). This area decreased by a half in 2021-2040 (Table 6) under both SSP245 and SSP585 scenarios. From current to future projections, the area occupied by G3 remains low and never exceeding 23ha.

Table 6. Change area from the currently to future time-periods according to the SSP245 and SSP585 scenarios from the CanESM5 model. G1: *Rhanterium suaveolens* and *Lygeum spartum*; G2: *Lycium shawii* and *Nitraria retusa*; G3*: Imperata cylindrica.*

		Area (ha)			Percent change (%)		
		G1	**G2**	**G3**	**G1**	**G2**	**G3**
2018	**Current**	146.85	77.46	19.50	0	0	0
2021-2040	**SSP245**	146.78	79.55	9.34	-0.05	2.70	-52.10
	SSP585	146.18	74.99	10.01	-0.46	-3.19	-48.67
2041-2060	**SSP245**	146.93	82.69	19.94	0.05	6.75	2.26
	SSP585	143.12	66.48	17.11	-2.54	-14.18	-12.26
2061-2080	**SSP245**	149.32	79.63	18.82	1.68	2.80	-3.49
	SSP585	145.28	68.20	21.96	-1.07	-11.95	12.62
2081-2100	**SSP245**	148.35	64.31	22.86	1.02	-16.98	17.23
	SSP585	146.85	76.71	22.04	0	-0.97	13.03

4. CONCLUSION

Maxent model is used to predict the potential distribution of plant groups and SAVI classes under different climate change scenarios in Zarat, coastal protected area of southern Tunisia. The results highlight the effectiveness of SAVI as reliable index for predicting the dynamic of vegetation within protected areas. The differences in response of the studied plant groups to the climatic scenarios can be linked to their floristic composition basically the tolerant species. Furthermore, the present work emphasizes the importance of studying plant group communities in order to accurately predict ecosystem functioning in the future climate scenarios. By using SAVI and plant group occurrences, researchers and conservationists can make informed decisions and take proactive measures to ensure the preservation and sustainability of protected areas and their ecosystems.

ACKNOWLEDGMENT

Many thanks are addressed to the anonymous reviewers for their valuable contributions and recommendations to fine-tune this manuscript.

REFERENCES

Almutairi, B., El, A., Belaid, M. A., Musa, N. (2013). Comparative Study of SAVI and NDVI Vegetation Indices in Sulaibiya Area (Kuwait) Using Worldview Satellite Imagery. *International Journal of Geosciences and Geomatics*, 1, 50-53.

Ben Mariem, H., Chaieb, M. (2017). Climate change impacts on the distribution of *Stipa tenacissima* L. ecosystems in north African arid zone--a case study in Tunisia. *Applied Ecology & Environmental Research*, 15(3).

Chen, T., Tang, G., Yuan, Y., Guo, H., Xu, Z., Jiang, G., Chen, X. (2020). Unraveling the relative impacts of climate change and human activities on grassland productivity in Central Asia over last three decades. *Science of the Total Environment*, 743, 140649.

Ding, H., Chiabai, A., Silvestri, S., Nunes, P. A. (2016). Valuing climate change impacts on European forest ecosystems. *Ecosystem Services* 18, 141-153.

Dülgeroğlu, C., Aksoy, A. (2019). Assessing impacts of climate change on Campanula yaltirikii H. Duman (Campanulaceae), a critically endangered endemic species in Turkey. *Turkish Journal of Botany*, 43(2), 243-252.

Erb, K.H., Kastner, T., Plutzar, C., Bais, A.L.S., Carvalhais, N., Fetzel, T., Gingrich, S., Haberl, H., Lauk, C., Niedertscheider, M., Pongratz, J. (2018). Unexpectedly large impact of forest management and grazing on global vegetation biomass. *Nature* 553,73-76.

Gann, G.D., McDonald, T., Walder, B., Aronson, J., Nelson, C.R., Jonson, J., Hallett, J.G., Eisenberg, C., Guariguata, M.R., Liu, J. and Hua, F., (2019). International principles and standards for the practice of ecological restoration. *Restoration Ecology*, 27, S1-S46.

Gao, W., Zheng, C., Liu, X., Lu, Y., Chen, Y., Wei, Y., Ma, Y. (2022). NDVI-based vegetation dynamics and their responses to climate change and human activities from 1982 to 2020: A case study in the Mu Us Sandy Land, China. *Ecological Indicators*, 137, 108745.

Ge, W., Deng, L., Wang, F., Han, J. (2021). Quantifying the contributions of human activities and climate change to vegetation net primary productivity dynamics in China from 2001 to 2016. *Science of the Total Environment*, 773, 145648.

Genin, D., Guillaume, H, Ouessar M., Ouled Belgacem, A., Romagny, B., Sghaier, M., Taamallah, H. (2006). Entre desertification et developement: la Jeffara tunisienne [Between desertification and development: The Tunisian Jeffara]. In: Ceres, editors. Tunis: IRA-IRD; p.1 – 351.

Huete, A. R. (1988). A soil-adjusted vegetation index (SAVI)', *Remote Sensing of Environment* 25, 295-309.

Jewitt, D., Goodman, P. S., Erasmus, B. F., O'Connor, T. G., Witkowski, E. T. (2015). Systematic land-cover change in KwaZulu-Natal, South Africa: Implications for biodiversity. *South African Journal of Science*, 111(9-10), 01-09.

Kumar, R. (2022). Remote sensing and GIS-based land use and land cover change detection mapping of Jind District, Haryana. Journal homepage: www. ijrpr. com ISSN, 2582, 7421.

Lemenkova, P., Debeir, O. (2023). Computing Vegetation Indices from the Satellite Images Using GRASS GIS Scripts for Monitoring Mangrove Forests in the Coastal Landscapes of Niger Delta, Nigeria. *Journal of Marine Science and Engineering*, 11: 871.

Lobo, J.M., Jiménez-Valverde, A., Real, R. (2008). AUC: A misleading measure of the performance of predictive distribution models. *Global Ecology and Biogeography*. 2008, 17, 145–151.

Lü, Y., Fu, B., Feng, X., Zeng, Y., Liu, Y., Chang, R., Sun, G., Wu, B. (2012). A policy-driven large

scale ecological restoration: quantifying ecosystem services changes in the Loess Plateau of China. *PLOS One*, 7(2), p.e31782.

Maina, J., Wandiga, S., Gyampoh, B., Charles, K. K. G. (2020). Assessment of land use and land cover change using GIS and remote sensing: A case study of Kieni, Central Kenya. *Journal of Remote Sensing & GIS*, 9(01), 1-5.

Massada, A. B., Syphard, A. D., Stewart, S. I., Radeloff, V. C. (2012). Wildfire ignition-distribution modelling: a comparative study in the Huron–Manistee National Forest, Michigan, USA. *International Journal of Wildland Fire*, 22(2), 174-183.

Medini-Bouaziz, L., El Gtari, M., Hamaied, S., Charfi-Cheikhrouha, F. (2017). Population dynamics and reproductive aspects of Porcellio albinus (Isopoda, Oniscidea) of Zarat (Gabes, Tunisia). *Invertebrate reproductIon & development* 61(1), 18-26.

Ouled Belgacem, A., Louhaichi, M. (2013). The vulnerability of native rangeland plant species to global climate change in the West Asia and North African regions. *Climatic Change*, 119, 451 – 463.

Parmesan, C., Yohe, G. (2003). A globally coherent fingerprint of climate change impacts across natural systems. *Nature* 421: 37–42.

Phillips, S.J., Dudik, M., Schapire, R.E. (2004). A maximum entropy approach to species distribution modeling'. In: Proceedings of the Twenty-First International Conference on Machine Learning; Banff, AB, Canada. p. 655-662

Piri Sahragard, H., Ajorlo, M. (2018). A comparison of logistic regression and maximum entropy for distribution modeling of range plant species (a case study in rangelands of western Taftan, southeastern Iran). *Turk J Bot* 42: 28-37.

Tarhouni, M., Ben Hmida, W., Ouled Belgacem, A., Louhaichi, M., Neffati, M. (2017). Is long-term protection useful for the regeneration of disturbed plant communities in dry areas? *African Journal of Ecology*, 55(4), 509-517.

Tong, L., Liu, Y., Wang, Q., Zhang, Z., Li, J., Sun, Z., Khalifa, M. (2019). Relative effects of climate variation and human activities on grassland dynamics in Africa from 2000 to 2015. *Ecological Informatics*, 53, 100979.

Xue, J., Su, B. (2017). Significant remote sensing vegetation indices: A review of developments and applications. *Journal of Sensors* 2017.

Yost, A. C., Petersen, S. L., Gregg, M and Miller, R. (2008). Predictive modeling and mapping sage grouse (Centrocercus urophasianus) nesting habitat using Maximum Entropy and a long-term dataset from Southern Oregon. *Ecological Informatics*, 3: 375-386.

Zeng, Y., Hao, D., Huete, A., Dechant, B., Berry, J., Chen, J. M., Joiner, J., Frankenberg, C., Bond-Lamberty, B., Ryu, Y. and Xiao, J. (2022). Optical vegetation indices for monitoring terrestrial ecosystems globally. *Nature Reviews Earth & Environment*, 3: 477-493.

Zhang, R., Liang, T., Guo, J., Xie, H., Feng, Q., Aimaiti, Y. (2018). Grassland dynamics in response to climate change and human activities in Xinjiang from 2000 to 2014. *Scientific Reports*, 8, 2888.

Zhao, Y., Cao, H., Xu, W., Chen, G., Lian, J., Du, Y., Ma, K. (2018). Contributions of precipitation and temperature to the large-scale geographic distribution of fleshy-fruited plant species: Growth form matters. *Scientific Reports*, 8(1), 17017.

Zhong, L., Ma, Y., Salama, M.S., Su, Z. (2010). Assessment of vegetation dynamics and their response to variations in precipitation and temperature in the Tibetan Plateau. *Climate Change*. 103, 519–535.